



The Comparative Assessment of the Quality of Cytological Drugs Image Processing

Hennadii Khudov¹, Olesya Symkanych², Anna Kovalenko³,
Natalia Kabus⁴, Viktor Lysytsya⁵, Rostyslav Khudov⁶,

¹Department of Radar Troops Tactic, Ivan Kozhedub Kharkiv National Air Force University, Kharkiv, Ukraine,
2345kh_hg@ukr.net

²Department of Pharmaceutical Disciplines, Uzhhorod National University, Uzhhorod, Ukraine,
olesjasi123@gmail.com

³Department of Cybersecurity and Software, Central Ukrainian National Technical University,
Kirovohrad, Ukraine, annasun911@gmail.com

⁴Department of Fundamental General Scientific Disciplines, Kharkiv International Medical University, Kharkiv,
Ukraine, kabusnatali9901@gmail.com

⁵Department of Higher Mathematics and Information Science, V. N. Karazin Kharkiv National University,
Kharkiv, Ukraine, lysytsya@karazin.ua

⁶Department of Theoretical and Applied Informatics, V. N. Karazin Kharkiv National University, Kharkiv,
Ukraine, rhudov@gmail.com

ABSTRACT

The features of cytological images during processing by automated microscopy systems are determined. The essence of the known methods of processing of cytological images used in algorithms of automatic selection and transformation of micro-objects on cytological images is briefly stated. The results of cytological image processing by k-means, Prewitt, Sobel, Canny, Hough methods and combinations of these methods are presented. A comparative visual and quantitative assessment of the quality of cytological image processing was performed. Errors of the first and second kind are selected as indicators of quality of cytological drugs image processing.

Key words: image, medicine, cytological drug, automated microscopy systems, method, cell, processing.

1. INTRODUCTION

At verification of the previous diagnosis and the subsequent treatment the cytological images of the investigated samples received by means of a microscope are used [1]–[4]. Cytological images are colour images of groups of cells of living organisms that contain similar micro-objects (in the absence of pathology) with weakly expressed contours, the colour range of which depends on the dyes used [1], [5]–[6].

The analysis of cytological images consists of operations of selection of micro-objects, definition of their characteristic features and an estimation of the received characteristics by the doctor. Automated microscopy systems are used to increase the speed of sample processing and reduce the influence of the human factor on the diagnostic results

[6]–[8]. The advantages of using automated microscopy systems are the ability to adjust the operating modes depending on tasks and minimizing the error of selection of micro-objects during the detection of precancerous conditions. Analysis of existing automated microscopy systems showed the absence of algorithms for automatic selection and conversion of micro-objects to cytological images. The development and verification of such methods is complicated by the peculiarities of cytological images and the limited size of test samples.

1.1 Problem analysis

Three approaches are used to select micro-objects in automated microscopy systems: manual, automated, and automatic [7]–[8]. Automatic and automated selection is based on the using of digital image segmentation algorithms [9]–[15].

The papers [7]–[8] present:

- the method of segmentation of color cytological images on the basis of previous markings, which, in contrast to the existing ones, combines several different criteria for assessing the homogeneity of areas;
- the method of automatic selection of the algorithm of segmentation of cytological images on the basis of the analysis of criteria of an estimation of homogeneity of areas and the analysis of the histogram of distribution of brightness by means of methods of fuzzy logic.

The methods [7]–[8] improved the accuracy of finding micro-objects in the images and provided minimal error in splitting the input image.

The paper [16] presents an approach to detect lung cancer in scanned images. The steps involved in it is proposed using methods of image preprocessing where median filter is used followed by segmentation here mathematical morphological operations are used. Geometrical features like area, perimeter, and eccentricity are calculated to tumor detected part. At last SVM classifier is used to classify whether it is cancerous (Malignant) or normal (Benign).

The papers [17]–[18] propose to use images of cytological preparations using wavelet transform. The visual quality of the image after conversion does not allow to identify all the cells. Further improvement of image quality requires additional pre-processing, which increases processing time and affects the final image processing quality.

Analysis of known segmentation methods showed that there is no universal algorithm for dividing the image into homogeneous regions, which leads to the dependence of the error of the segmentation results on the characteristics of the image itself. Among the analyzed contouring algorithms, the dependence of the results of their work on the choice of stop criteria and re-checking of some points of the image, which slows down the algorithms, was investigated.

Analysis of skeleton-based transformation methods [19]–[20] has shown insufficient accuracy of known image conversion algorithms.

The growing demands on the efficiency and accuracy of the analysis results in the need to create new and improve existing methods and algorithms for the analysis of cytological images. Therefore, the task of developing methods is important and relevant to increase the accuracy of processing cytological images in automated microscopy systems and to compare of these methods.

The aims of the paper are: a brief description of the essence of the known methods of automated processing of cytological images, a comparative visual and quantitative assessment of the quality of processing of cytological images.

2. MAIN MATERIAL

The cytological images are characterized by low contrast, which makes it difficult to distinguish objects on them. The increasing the reliability of the results of segmentation of cytological objects is achieved by determining the specific properties of individual objects. This is highly individualized and cannot be applied to analysis of cytological images in general. There are two main directions for solving this problem. The first is based on the specific processing of individual classes of objects, leading to the use of highly specialized tools. The second is on the determination of the general properties of objects, the selection of large general classes. This direction gives a lower quality result, but allows

you to define large classes of objects. It is more promising, as it helps to expand the range of tasks to be solved.

On cytological images, four main classes of objects: fragments of fabric (texture objects); vessels and fibers in longitudinal section (extended objects); cells, nuclei, vessels and fibers in cross section (convex objects); cellular inclusions and nucleoli (small contrasting objects). Let's briefly consider the main methods of processing cytological images.

I. The iterative algorithm of k-means clustering is often used when processing color and grayscale images [12], [15], [21]. It is based on minimizing the squared error (expression (1)):

$$V = \sum_{i=1}^K \sum_{x \in C_i} (x - \mu_i)^2 . \quad (1)$$

The goal of the algorithm is to divide the original image of N pixels into K clusters. A cluster is a certain grouping of pixels that depends on the values of pixels in the image, but does not depend on their location in the original image. Such dependence appears when the coordinates of pixels are a given property of pixels that is important for clustering.

Let $X = \{x_1, \dots, x_N\}$ – a set of N pixels of the image, $V(x_i)$ – a vector of properties associated with a pixel x_i . The k-means clustering consists of the following steps (Figure 1):

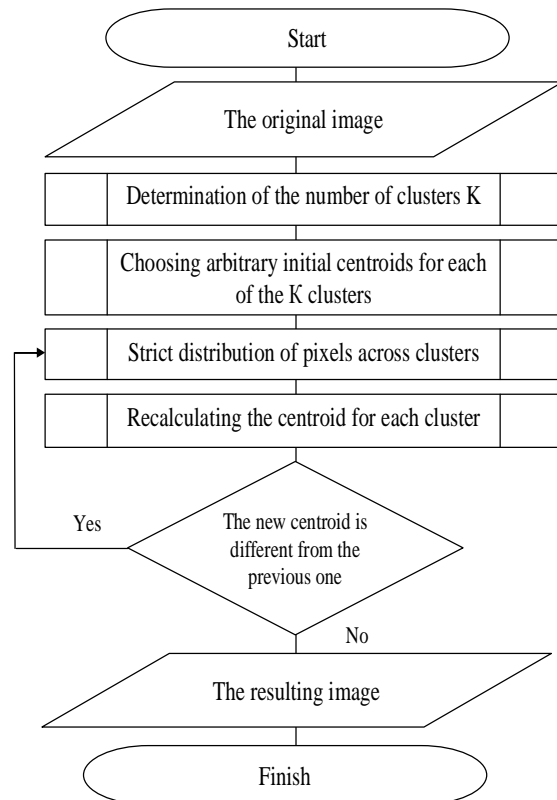


Figure 1. Steps of algorithm of k-means clustering

1. The determination of the number of clusters K by the user randomly or based on some heuristic.

2. The choice of arbitrary initial centroids for each of the K clusters.

In the classical k-means clustering, the value of each element $V(x_i)$ is chosen at random from the set of all possible values for that element. For example, if a property vector has the form (R,G,B) and represents the intensity of red, green, and blue, respectively, the first element R will be selected at random from all possible intensities of red.

3. Strict distribution of pixels across clusters.

When each of the K clusters C_k has a centroid μ_k , then all pixels are added to the cluster with the nearest centroid. Adding a pixel to a cluster is based on a distance function that defines the distance between two vectors of properties. After that, each pixel x_i belongs to only one cluster C_k .

4. Recalculate the centroid for each cluster.

The cluster centers are recalculated. For this, the value of the vectors of properties of all pixels in each cluster is used. Thus, the centroid μ_k is calculated as follows by expression (2):

$$\{V(x_i) | x_i \in C_k\}. \tag{2}$$

Steps 3 and 4 are iteratively repeated until the centers of the clusters stop changing. Obviously, that the boundaries of the clusters change and their centers shift at each iteration. As a result, the distance between elements within clusters is minimized and inter-cluster distances are increased. The algorithm will stop when the boundaries of the clusters and the location of the centroid do not stop changing and the pixels will remain in the same cluster at the next iteration. This is called convergence. The main advantages are ease of implementation and speed of work. It does a good job of clustering pixels in an image, but in the process of image processing it cannot exclude unnecessary information, such as, for example, noises of various kinds. Also, there may be erroneous results for highlighting areas in colour images using the k-means clustering. Namely, areas with different colours and the same intensity can merge.

II. Operators by Sobel, Prewitt, and Robert are classified as classical operators, which are easy to implement but highly sensitive to noise [15], [22]–[23]. The principle of operation of such an algorithm for such classical operators is shown in Figure 2.

These gradient methods are based on the selection of edge points, which, insensitive to noise and contrast images. They are based on the property luminance signal – discontinuity. Effective the way to find breaks is to handle images with a sliding mask - spatial filtering. During this filtering, the filter mask moves from pixel to pixel. For detecting brightness

differences are used discrete analogues of the derivatives of the first and second orders.

Like the Sobel operator, the Prewitt operator is also used to detect two kinds of edges in an image: G_x – vertical direction;

G_y – horizontal direction.

The main difference is that the Sobel operator's coefficients of mask are not fixed and can be adjusted according to our requirements, as long as they do not violate any property of the derived masks.

The Sobel edge detection method consists of the following steps (Figure 3):

1. Convolution of the original image with a 3x3 kernel to calculate the approximate values of the vertical and horizontal derivatives.

Let A – the original image, G_x and G_y – two images in which the point contains the approximate derivatives with respect to x and y . They are calculated by the following expressions (3) and (4):

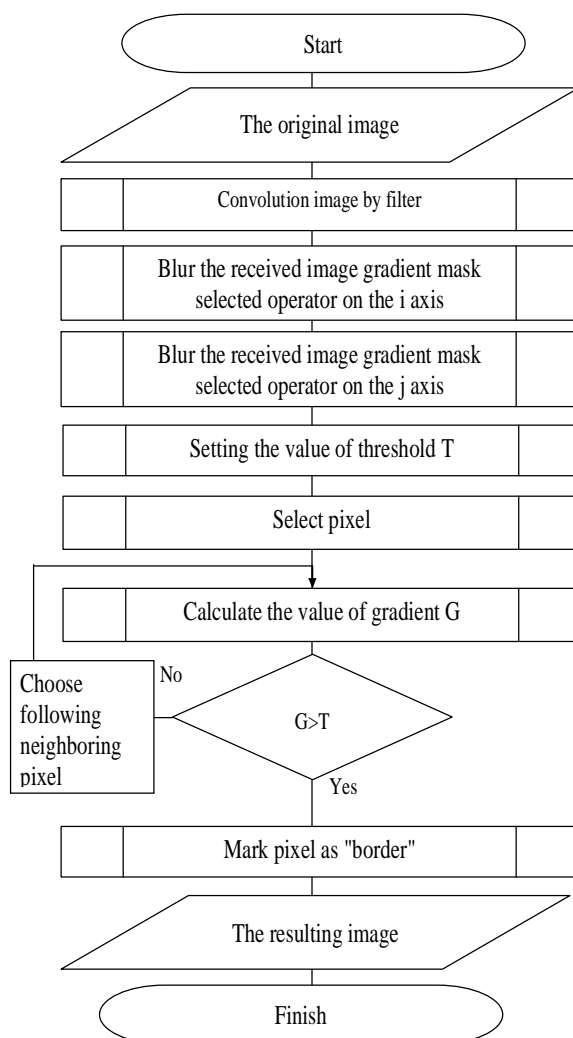


Figure 2. The basic principle of the algorithm for such classical gradient operators

$$G_x = \begin{bmatrix} -1 & 0 & 1 \\ -2 & 0 & 2 \\ -1 & 0 & 1 \end{bmatrix} * A; \tag{3}$$

$$G_y = \begin{bmatrix} -1 & -2 & -1 \\ 0 & 0 & 0 \\ 1 & 2 & 1 \end{bmatrix} * A, \tag{4}$$

where * – two-dimensional convolution.

2. Calculating the gradient G. The approximate value of the gradient G at each point of the image is calculated. The value of the gradient G can be calculated by element-wise use of the obtained approximate values of the derivatives (expression 5):

$$G = \sqrt{G_x^2 + G_y^2}, \tag{5}$$

or using the following simplification (expression 6):

$$G = |G_x| + |G_y|, \tag{6}$$

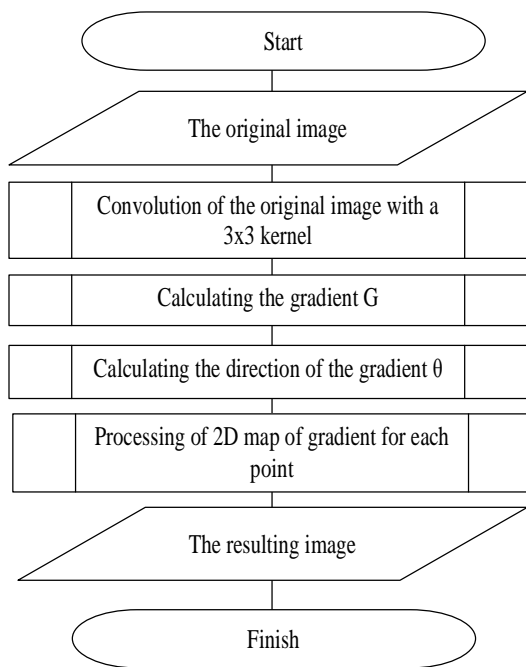


Figure 3. Steps of the Sobel edge detection method

3. Calculating the direction of the gradient θ (expression 7):

$$\theta = \arctg\left(\frac{G_x}{G_y}\right), \tag{7}$$

where, for example, $\theta = 0$ for a vertical border that has a left side.

4. Processing of 2D map of gradient for each point. The result of the Sobel operator is a two-dimensional map of gradient for each point. It can be processed and shown as a picture in which areas with a large gradient value (mainly edges) will be visible as white lines.

The disadvantage of the Sobel operator is the lack of rotational symmetry in matrices for calculating the values of the approximate derivatives in the vertical and horizontal directions. This leads to the loss of some contours.

Since there are no fixed coefficients in the Sobel operator, more weight can be applied to the mask. The more weight the mask has, the more edges it will highlight. The main disadvantage of the Sobel operator is the high computation time compared to the same Robert operator.

The Prewitt operator is very similar to the Sobel operator. It is also a derived mask that is used for edge detection. The main difference is that the coefficients of the Prewitt operator mask are fixed, they cannot be corrected and the mask has the form calculated by the following expressions (8) and (9):

$$G_x = \begin{bmatrix} +1 & 0 & -1 \\ +1 & 0 & -1 \\ +1 & 0 & -1 \end{bmatrix} * A; \tag{8}$$

$$G_y = \begin{bmatrix} +1 & +1 & +1 \\ 0 & 0 & 0 \\ -1 & -1 & -1 \end{bmatrix} * A, \tag{9}$$

To solve the question of invariance, both the Sobel and Prewitt methods with respect to rotation use the diagonal components of the gradient G_{yx} and G_{xy} . For example, kernels G_x and G_y will be as follows (expressions (10) and (11)):

$$G_{xy} = \begin{bmatrix} +1 & +1 & 0 \\ +1 & 0 & -1 \\ 0 & -1 & -1 \end{bmatrix}; \tag{10}$$

$$G_{yx} = \begin{bmatrix} -1 & -1 & 0 \\ -1 & 0 & +1 \\ 0 & +1 & +1 \end{bmatrix}; \tag{11}$$

The Sobel operator has a large kernel, which makes the operator less susceptible to noise. Local averaging is performed in the vicinity of the mask due to the large size possibility. This reduces errors from noise exposure.

III. The papers [6], [24]–[26] presents the Canny method. The Canny method consists of the following steps (Figure 4) [6].

IV. The paper [6] presents two-stages method. The first stage is the selection of contours using any edge detection algorithm. The second stage is the selection of geometric primitives using the Hough transform [6], [27]–[30].

2.1 Experimental research

There is the original image (Figure 5 [1]). This image was taken from Carl Zeiss microscope. The Figure 5 shows the bone marrow cells that need to be identified. The Figure 6 shows the fragment of Figure 5, where the bone marrow cells intersect. This certainly complicates the task of automated detection of bone marrow cells.

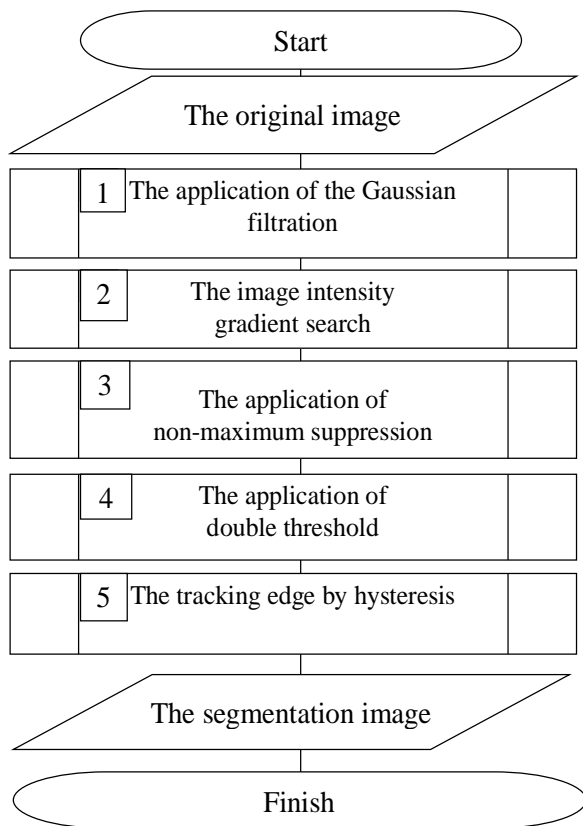


Figure 4. The steps of the Canny method

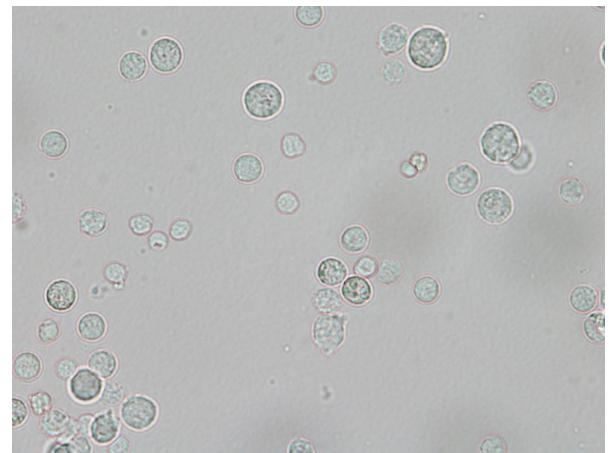


Figure 5. The original image [1]

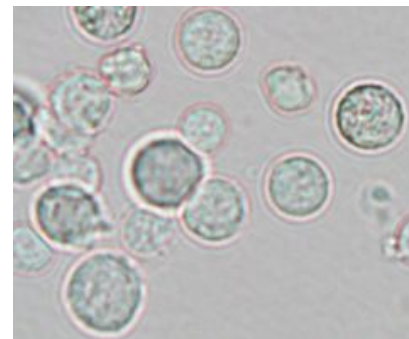
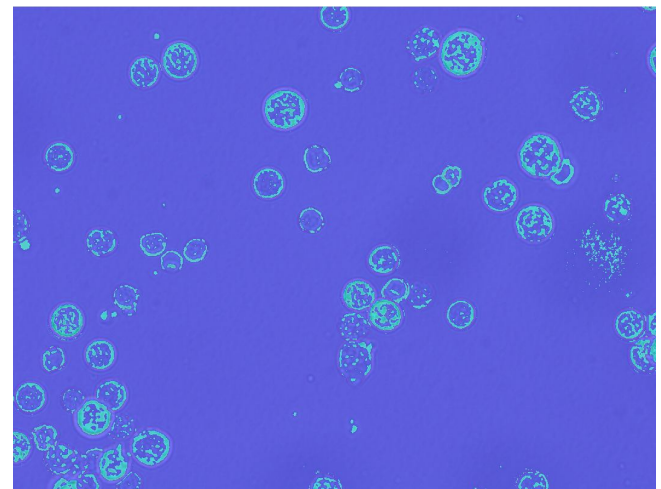
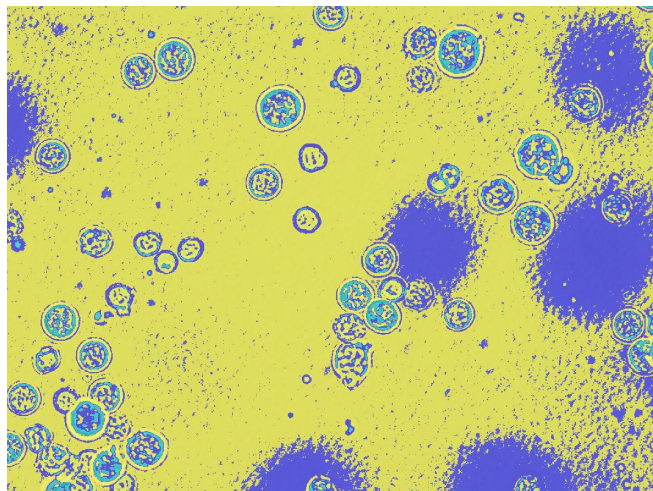


Figure 6. The fragment of Figure 5, where the bone marrow cells intersect

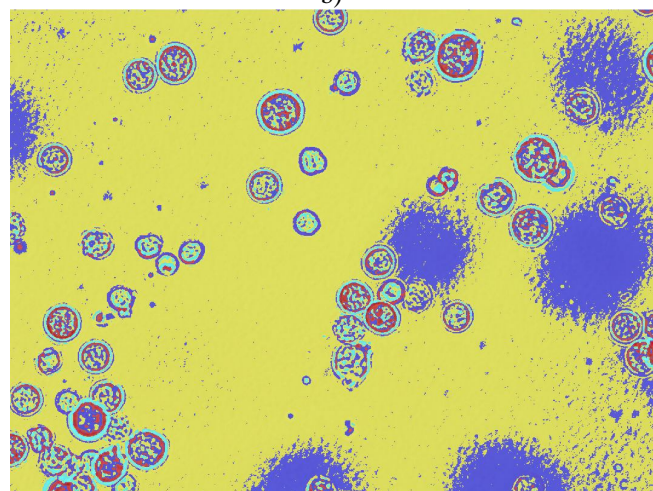
The results of applying of k-means method to Figure 5 are shown in Figure 7,a,b,c for k=2 (Figure 7a), for k=3 (Figure 7b), for k=4 (Figure 7c).



a)



b)



c)

Figure 7. The results of applying k-means method to the original image (Figure 5): a) k=2; b) k=3; c)k=4

The results of applying of Sobel, Prewitt and Canny methods to Figure 5 are shown in Figure 8, Figure 9 and Figure 10 respectively.

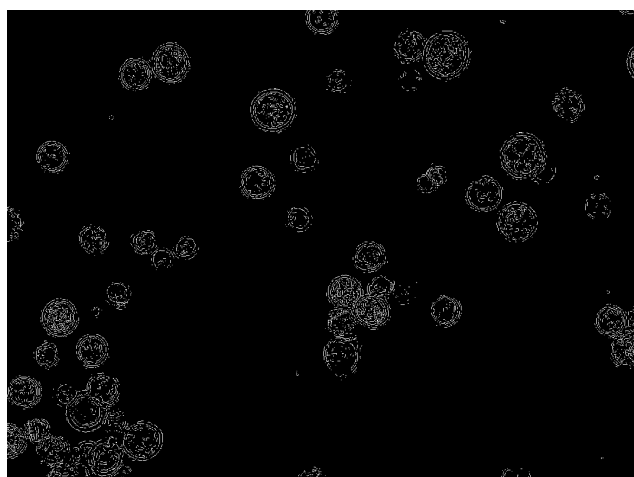


Figure 8. The result of applying of Sobel method to the original image (Figure 5)

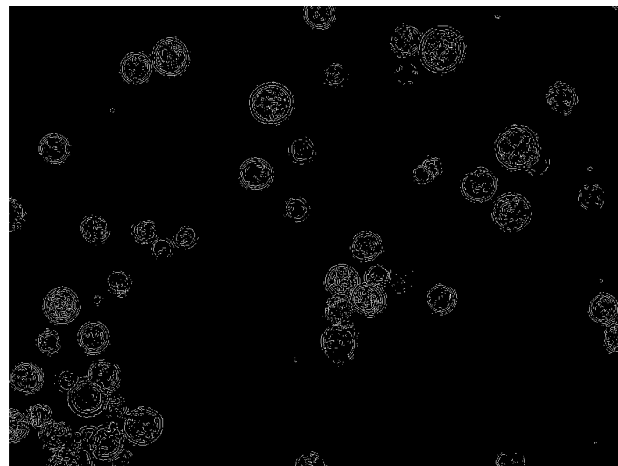


Figure 9. The result of applying of Prewitt method to the original image (Figure 5)

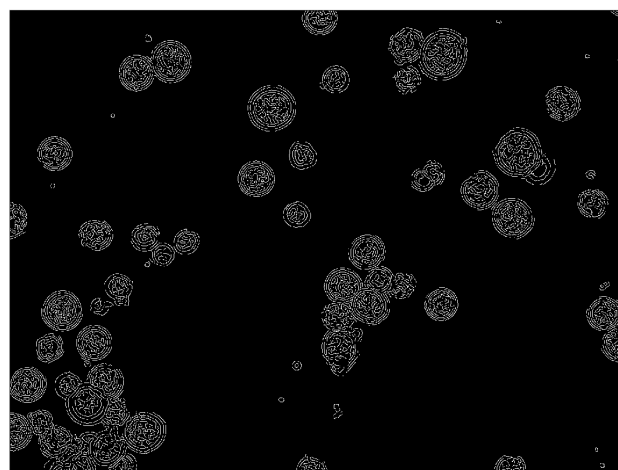


Figure 10. The result of applying of Canny method to the original image (Figure 5)

The result of applying of Hough transformation method to Figure 5 is shown in Figure 11.

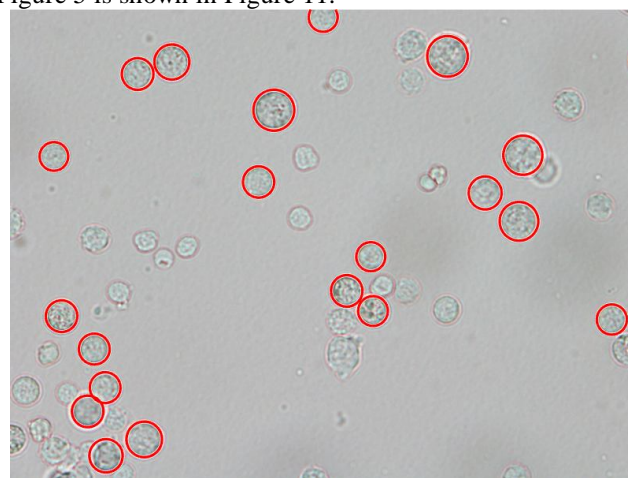


Figure 11. The result of applying of Sobel method to the original image (Figure 5)

The results of applying of two-stages methods [6] to Figure 5 are shown in Figure 12, Figure 13 and Figure 14.

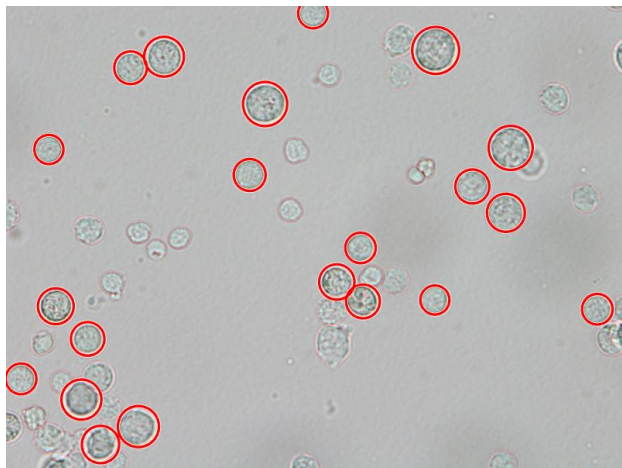


Figure 12. The result of applying of two-stages method [6] to the original image (Figure 5) (the first stage is Sobel method)

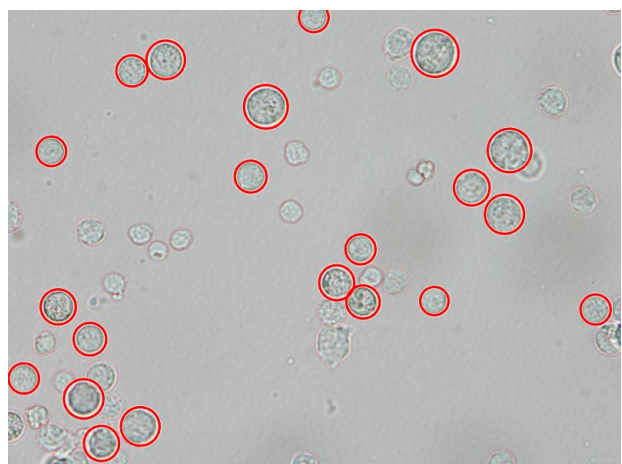


Figure 13. The result of applying of two-stages method [6] to the original image (Figure 5) (the first stage is Prewitt method)

The first stages for two-stages methods are: Sobel method. (Figure 12), Prewitt method (Figure 13) and Canny method (Figure 14).



Figure 14. The result of applying of two-stages method [6] to the original image (Figure 5) (the first stage is Canny method)

The visual quality of the processed cytological images indicates the advisability of choosing two-stage methods. In this case, the most suitable is the two-stage method, when the Canny method is used at the first stage, and the Hough transformation for circles is used at the second stage (Figure 14).

The indicators for determining the quality of cytological drugs image processing shall be errors of first and second kind. The errors of determination of bone marrow cells of first (α_1) and second (β_2) kind are determined based on the maximum likelihood criterion, which follows from the generalized criterion of an average risk minimum [20]. The errors of determination of bone marrow cells of first kind α_1 and second kind β_2 are calculated from expressions (12), (13), respectively [20]:

$$\alpha_1 = \frac{S_1((fs(\mathbf{X})))}{S_2(f(\mathbf{X}))}, \tag{12}$$

$$\beta_2 = 1 - \frac{S_3(fs(\mathbf{X}))}{S_4((f(\mathbf{X})))}. \tag{13}$$

The values for first and second kind errors for different methods, calculated from expressions (16), (17), are given in Table 1.

Table 1 – The estimation of the first and second kind errors

	Sobel method		Prewitt method		Canny method	
	One stage	Two stage	One stage	Two stage	One stage	Two stage
$\alpha_1, \%$	37	23	31	19	22	16
$\beta_2, \%$	33	21	29	17	19	13

5. CONCLUSION

Thus, the visual quality and the values for first and second kind errors for different methods of the processed cytological images indicates the advisability of choosing two-stage methods. In this case, the most suitable is the two-stage method, when the Canny method is used at the first stage, and the Hough transformation for circles is used at the second stage.

REFERENCES

1. Roche Digital Diagnostics, URL: <https://diagnostics.roche.com/global/en/products/product-category/roche-digital-diagnostics0.html> (accessed 13 October 2020).
2. P. Yellamma1, Ch.Chowdary, G. Karunakar, B. Subba Rao, and V. Ganesan **Breast Cancer Diagnosis Using MLP Back Propagation**, *International Journal of Emerging Trends in Engineering Research*, Vol. 8. № 9, 2020, P. 5539–5544. DOI: <https://doi.org/10.30534/ijeter/2020/102892020>.

3. V. Pawar, K. Kharat, S. Pardeshi, and P. Pathak **Lung Cancer Detection System Using Image Processing and Machine Learning Techniques**, *International Journal of Advanced Trends in Computer Science and Engineering*, Vol. 9. № 4, 2020, P. 5956–5963. DOI: <https://doi.org/10.30534/ijatcse/2020/260942020>.
4. P. V. Kuzyk, M. A. Savchyna, S. G. Gychka **Rare case of nodular lymphoid hyperplasia of left lung in the patient with previous pulmonary tuberculosis**, *Experimental Oncology*, Vol. 40. № 4, 2018, P. 332–335. DOI: [https://doi.org/10.31768/2312-8852.2018.40\(4\):332-335](https://doi.org/10.31768/2312-8852.2018.40(4):332-335).
5. S. L. Ohiienko, A. Yu. Bondar, E. G. Ivanov, and I. A. Ionov **Bonemarrow cells obtained from old animals differ from the young animals cells in their ability to divide and in response to the presence of liver fibrosis in primary culture**, *Advances in Aging Research*. 2019. Vol. 8. P. 14–27.
6. H. Khudov, I. Ruban, V. Lysytsya, P. Kuzyk, O. Symkanych, and R. Khudov, **The Method for Determination of Bone Marrow Cells in Photographic Images**, *International Journal of Emerging Trends in Engineering Research*, Vol. 8. № 9, 2020, pp. 5681–5687. DOI: <https://doi.org/10.30534/ijatcse/2020/131892020>.
7. O. Berezsky, G. Melnyk, and Yu. Batko **Modern Trends in Biomedical Image Analysis System Design**, *Biomedical engineering trends in electronics, communications and software – Rijeka, Croatia: InTech*, 2011. P. 461–480.
8. O. Berezsky, G. Melnyk, and Y. Batko **Biomedical Image Search and Retrieval Algorithms**, *Computing*. № 7, 2008. P. 108–114.
9. I. Ruban, and H. Khudov, **Advances in Spatio-Temporal Segmentation of Visual Data, Chapter 2. Swarm Method of Image Segmentation**. *Series Studies in Computational Intelligence (SCI)*, Vol. 876. – Publisher Springer, Cham, 2020. – P. 53-99. DOI <https://doi.org/10.1007/978-3-030-35480-0>.
10. H. Khudov, S. Glukhov, V. Podlipaiev, V. Pavlii, I. Khizhnyak, and I. Yuzova **The Multiscale Image Processing Method from On-board Earth Remote Sensing Systems Based on the Artificial Bee Colony Algorithm** *International Journal of Advanced Trends in Computer Science and Engineering*, Vol. 9. № 3, 2020, P. 2557–2562. DOI: <https://doi.org/10.30534/ijatcse/2020/11932020>.
11. H. Khudov, R. Khudov, I. Khizhnyak, V. Loza, T. Kravets, S. Kibitkin **Estimation of the Kullback-Leibler Divergence for Canny Edge Detector of Optoelectronic Images Segmentation**, *International Journal of Emerging Trends in Engineering Research*, Vol. 8. № 7, 2020, pp. 3927–3934. DOI: <https://doi.org/10.30534/ijeter/2020/162872020>.
12. A. El-Baz, X. Jiang, and S. Jasjit (Eds.) **Biomedical image segmentation: advances and trends**. CRC Press, 2016. 546 p.
13. I. Ruban, V. Khudov, O. Makoveichuk, H. Khudov, and I. Khizhnyak. **A Swarm Method for Segmentation of Images Obtained from On-Board Optoelectronic Surveillance Systems**, in *Intern. Scient.-Pract. Conf. Problems of Infocommunications. Science and Technology (PIC S&T)*, 2018, pp. 613–618. DOI: <https://doi.org/10.1109/infocommst.2018.8632045>.
14. I. Ruban, H. Khudov, O. Makoveichuk, I. Khizhnyak, V. Khudov, V. Podlipaiev, V. Shumeiko, O. Atrasevych, A. Nikitin, and R. Khudov. **Segmentation of optoelectronic images from on-board systems of remote sensing of the Earth by the artificial bee colony method**, *Eastern-European Journal of Enterprise Technologies*, № 2/9 (98), 2019, pp. 37–45. DOI: <https://doi.org/10.15587/1729-4061.2019.161860>.
15. R. Gonzalez, and R. Woods, **Digital Image Processing. 4th Edition**. Prentice Hall, Upper Saddle River, 2017. 1192 p.
16. D. Nagajyothi, R. Addagudi, T. Gunda, S. Logitla, and G. Arun **Detection of Lung Cancer using SVM Classifier**, *International Journal of Emerging Trends in Engineering Research*, № 8(5), 2020, pp. 2177–2180. DOI: <https://doi.org/10.30534/ijeter/2020/113852020>.
17. V. V. Lyashenko, A. M. Babker, and O. A. Kobylin **Using the methodology of wavelet analysis for processing images of cytology preparations** *National Journal of Medical Research*. 2016. T. 6. № 1. P. 98–102.
18. V. V. Lyashenko, A. M. Babker, and O. A. Kobylin **The methodology of wavelet analysis as a tool for cytology preparations image processing** *Cukurova Medical Journal*. 2016. T. 41. № 3. C. 453–463.
19. R. Slama, H. Wannous, M. Daoudi, and A. Srivastava, **Accurate 3D action recognition using learning on the grassmann manifold**, *Pattern Recognit.* Vol. 48, № 2, 2015. P. 556–567.
20. P. Wang, W. Li, P. Ogunbona, J. Wan, and S. Escalera, **RGB-D-based human motion recognition with deep learning: A survey**, *Comput. Vis. Image Understand.* Vol. 171, 2018. P. 118–139.
21. Ruban I., Khudov H., Makoveychuk O., Khizhnyak I., Khudov V., and Lishchenko V. **The model and the method for forming a mosaic sustainable marker of augmented reality**. *Advanced Trends in Radioelectronics, Telecommunications and Engineering (TCSET): Thesis of 2020 IEEE 15th International Conference (Slavske, February 25–29, 2020)*. Slavske: IEEE, 2020. P. 402–406. DOI: <https://doi.org/10.1109/TCSET49122.2020.235463>.
22. I. Ruban, H. Khudov, O. Makoveichuk, M. Chomik, V. Khudov, I. Khizhnyak, V. Podlipaiev, Y. Sheviakov, O. Baranik, and A. Irkha. **Construction of methods for determining the contours of objects on tonal aerospace images based on the ant algorithms**, *Eastern-European Journal of Enterprise Technologies*, № 5/9 (101), 2019, pp. 25–34. DOI: <https://doi.org/10.15587/1729-4061.2019.177817>.

23. I. Ruban, V. Khudov, H. Khudov, and I. Khizhnyak **An Improved Method for Segmentation of a Multiscale Sequence of Optoelectronic Images**, in *Intern. Scient.-Pract. Conf. Problems of Infocommunications. Science and Technology (PIC S&T)*, 2017, pp. 137–140. DOI: <https://doi.org/10.1109/INFOCOMMST.2017.8246367>
24. J. F. Canny **Computational Approach to Edge Detection** *IEEE Transactions on Pattern Analysis and Machine Intelligence*. 1986. № 8. – P. 679–698.
25. A. Kabade, and V. Sangam **Canny edge detection algorithm** *International Journal of Advanced Research in Electronics and Communication Engineering (IJARECE)*. 2016. Vol. 5. Issue 5. P. 1292–1295.
26. H. Khudov, O. Makoveychuk, I. Khizhnyak, I. Yuzova , A. Irkha, and V. Khudov. **The Mosaic Sustainable Marker Model for Augmented Reality Systems**, *International Journal of Advanced Trends in Computer Science and Engineering*, Vol. 9. № 1, 2020, pp. 637–642. DOI: <https://doi.org/10.30534/ijatcse/2020/89912020>.
27. I. Ruban, H. Khudov, O. Makoveichuk, I. Khizhnyak, N. Lukova-Chuiko, G. Pevtsov, Y. Sheviakov, I. Yuzova, Y. Drob, and O. Tytarenko, **Method for determining elements of urban infrastructure objects based on the results from air monitoring**, *Eastern-European Journal of Enterprise Technologies*, № 4/9 (100), 2019, pp. 52–61. DOI: <https://doi.org/10.15587/1729-4061.2019.174576>.
28. A. Manzanera, T. Nguyen, and X. Xu **Line and circle detection using dense one-to-one Hough transforms on greyscale images** *EURASIP Journal on Image and Video Processing*, Springer. – 2016. № 34. P. 1773–2000.
29. H. Khudov, I. Ruban, O. Makoveichuk, H. Pevtsov, V. Khudov, I. Khizhnyak, S. Fryz, V. Podlipaiev, Y. Polonskyi, and R. Khudov. **Development of methods for determining the contours of objects for a complex structured color image based on the ant colony optimization algorithm**, *Eureka: Physics and Engineering*, № 1, 2020, pp. 34–47. DOI: <https://doi.org/10.21303/2461-4262.2020.001108>.
30. I. Ruban, O. Makoveichuk, V. Khudov, I. Khizhnyak, H. Khudov, I. Yuzova, and Y. Drob. **The Method for Selecting the Urban Infrastructure Objects Contours**, in *Intern. Scient.-Pract. Conf. Problems of Infocommunications. Science and Technology (PIC S&T)*, 2019, pp. 689–693. DOI: <https://doi.org/10.1109/infocommst.2018.8632045>.